

## Reflexion of a weak shock wave with vibrational relaxation

By CHING-MAO HUNG AND RICHARD SEEBASS

Cornell University, Ithaca, New York

(Received 4 October 1972 and in revised form 19 December 1973)

The structure of a shock wave in a vibrationally relaxing gas undergoing reflexion from a plane wall is examined. The shock wave is assumed to be weak, and departures from thermodynamic equilibrium are assumed small; both an adiabatic and an isothermal wall are considered. The flow field is divided into three regions: a far-field region, an interaction region, and, for the isothermal-wall case, a thermal boundary layer. Different asymptotic expansions are determined for the various regions through the method of matched asymptotic expansions. In the region far from the wall, a non-equilibrium Burgers equation governs the motion and the incident and the reflected shock wave structures. During reflexion, a non-equilibrium wave equation applies; its first-order terms are equivalent to an acoustic approximation. Heat conduction to the wall is modelled by an isothermal wall boundary condition which requires the introduction of a thermal boundary layer adjacent to the wall. This thermal boundary layer is thin and the adiabatic-wall result provides the outer solution for treating this layer. This thermal layer affects the structure of the reflected wave.

---

### 1. Introduction

The thermodynamic equilibrium that normally exists between the various forms of energy of gas molecules may be temporarily destroyed by the sudden change of temperature that occurs when a gas is traversed by a shock wave. While translational and rotational degrees of freedom return to equilibrium after a few collisions, some of the internal degrees of freedom may require hundreds or thousands of collisions before they readjust to thermodynamic equilibrium. In many polyatomic molecules, energy is invested in the vibrational mode, even when the gas is processed by an acoustic wave or a weak shock. Determining the amount of energy invested in the vibrational mode is important in sound absorption, moderately high enthalpy internal and external flows, and in other situations (see e.g. Freeman 1958; Vincenti & Kruger 1965; Glassman 1966; Becker 1970). An account of the basic physics of such processes, as well as their effect on basic gasdynamic flows, was given by Clarke & McChesney (1964).

A shock wave heats the gas passing through it rapidly and homogeneously, and thus provides a useful experimental means of initiating non-equilibrium processes. However, the gas processed by a shock wave is set in motion, complicating experimental measurements. Allowing the shock wave to reflect from the

end wall of a shock tube results in a nearly quiescent gas, and provides some advantages in studying the non-equilibrium rates. Spence (1961) was the first to study analytically the unsteady flow field behind a reflected shock wave in a relaxing gas. He investigated the motion of a strong shock wave produced by a piston and pointed out that relaxation times could be measured by observing the shock path. Baganoff (1965) measured the end-wall pressure histories in shock-reflexion processes, and concluded that the end-wall pressure, which is easy to measure, is quite sensitive to the relaxation processes in the driven gas. The method of characteristics has been employed to calculate the reflected shock-wave flow field in the presence of relaxation; Johannesen, Bird & Zienkiewicz (1967) combined the Rankine-Hugoniot, characteristic, and Rayleigh-line equations, and made calculations for vibrational relaxation in carbon dioxide. They found good agreement among computer results, Baganoff's end-wall pressure histories and their own experimental results of density distribution behind the reflected shock. Presley & Hanson (1968) also employed the method of characteristics and carefully calculated the time-dependent reflected shock-wave flow field with chemical reaction. Later, Hanson (1971*a, b*) used this concept, employed the approximate large-time and small-time solutions for the end-wall pressure history to establish the timewise variations of the thermodynamic state of the gas adjacent to the wall, and used these results to study vibrational relaxation in carbon monoxide. Brandon (1969) calculated shock-wave reflexion with vibrational relaxation behind the incident shock wave and simultaneous chemical and vibrational relaxation behind the reflected shock wave.

Goldsworthy (1959) determined the effect of end-wall heat transfer on the trajectory of a reflected shock wave; Clarke (1967) modified this result by allowing temperature jump at the end wall. This effect was easily observed in the experiments of Sturtevant & Slachmuylders (1964) and Baganoff (1965), who compared their measurements with Goldsworthy's theory. Later, Lesser & Seebass (1968) determined the effect of an isothermal wall boundary condition on the structure of a weak shock wave.

Buggisch (1969) delineated the analytical solution for the case when the shock is weak but vibrational effects are strong relative to the shock strength; Buggisch (1970) considered the case of a relatively strong shock perturbed by weak vibrational effects. He did not consider the effect of heat transfer to the end wall. The theory we present here considers the case of a weak shock when the effects of vibrational relaxation are of the same order as the shock strength. We also include the important effect of heat transfer to the end wall.

In this paper we assume that the shock wave is weak, but that it is still able to excite the gas vibrationally, that the state is one of small departure from thermodynamic equilibrium, and therefore that a simple rate model is appropriate. The shock wave is assumed fully formed long before reflexion occurs, so that it is steady with respect to shock-fixed co-ordinates, and its structure can be calculated from the governing equations. Such a steady solution provides the initial conditions for the wall-reflexion problem.

The linear theory of wave propagation in a relaxing gas concludes that at large times the shock structure will be diffusive in character, centred on the equilibrium

characteristic, and will occupy a region whose width grows parabolically with time or with distance from the origin. This is not the asymptotic behaviour that would be expected physically for the far-field steady shock wave. Blythe (1969) and Ockendon & Spence (1969) developed the appropriate nonlinear theory, and showed that a generalization of the Burgers equation to the case of a relaxing gas applies. Analogous to the Burgers equation, this 'non-equilibrium Burgers equation' applies only to waves moving in one direction.

In the absence of heat conduction, reflexion from a plane wall is analogous to two shock waves of opposite families interacting with each other. Consequently, to treat the reflexion process, we need an equation which takes account of wave motion in two directions; such an equation is derived here. The first-order solution implies an acoustic approximation. When heat conduction to the end wall is significant (as it usually is after some time), a thin thermal layer arises and must be treated separately. The method of matched asymptotic expansions is used to provide solutions in adjacent domains. For an adiabatic wall, the expansion is carried out in a parameter that is a measure of the shock strength. For an isothermal wall there is an additional parameter related to the heat diffusivity of the gas. For many shock-tube experiments, wall heat conduction is sufficient to ensure a nearly isothermal wall if the incoming shock is weak.

There are two cases to consider, depending upon the magnitude of the Mach number  $M_{f_0}$  based on the frozen sound speed. For  $M_{f_0} < 1$ , the incoming shock wave is fully dispersed; for  $M_{f_0} > 1$ , the incoming shock wave is partly dispersed.

The methods used here are analogous to those used by Lesser & Seebass (1968) in their study of the structure of a weak shock wave undergoing reflexion from a wall. In §2 we formulate the problem and determine the incoming shock structure; in §3 we determine the solution for reflexion from an adiabatic wall. In §4 we make the necessary modifications for an isothermal wall. A numerical method is employed to determine the effect of the velocity induced by the thermal layer on the reflected-shock trajectory and flow structure. In §5 we discuss our results.

## 2. Formulation and incoming shock structure

As indicated in figure 1, we consider a shock wave whose amplitude is measured by the speed  $u^*$  of the gas behind the shock propagating from the left in a semi-infinite uniform fluid initially at rest with pressure  $p_0^*$ , density  $\rho_0^*$ , translational and rotational temperature  $T_0^*$ , internal temperature  $T_i^*$ , and the corresponding frozen and equilibrium sound speeds,  $a_{f_0}$  and  $a_{e_0}$ , respectively. The undisturbed fluid is assumed to be in equilibrium state; that is,

$$T_0^* = T_i^* \quad \text{and} \quad u^* = 0.$$

The shock strength as measured by  $u^*/a_{f_0}$  is assumed weak ( $u^*/a_{f_0} \equiv \epsilon \ll 1$ ); far from the wall, the incident shock wave has a steady-state structure, which propagates at a constant shock speed  $U_0^*$ . Long after reflexion, the structure of the reflected shock wave will once again approach a steady state determined by the incident shock strength and the equilibrium thermodynamic

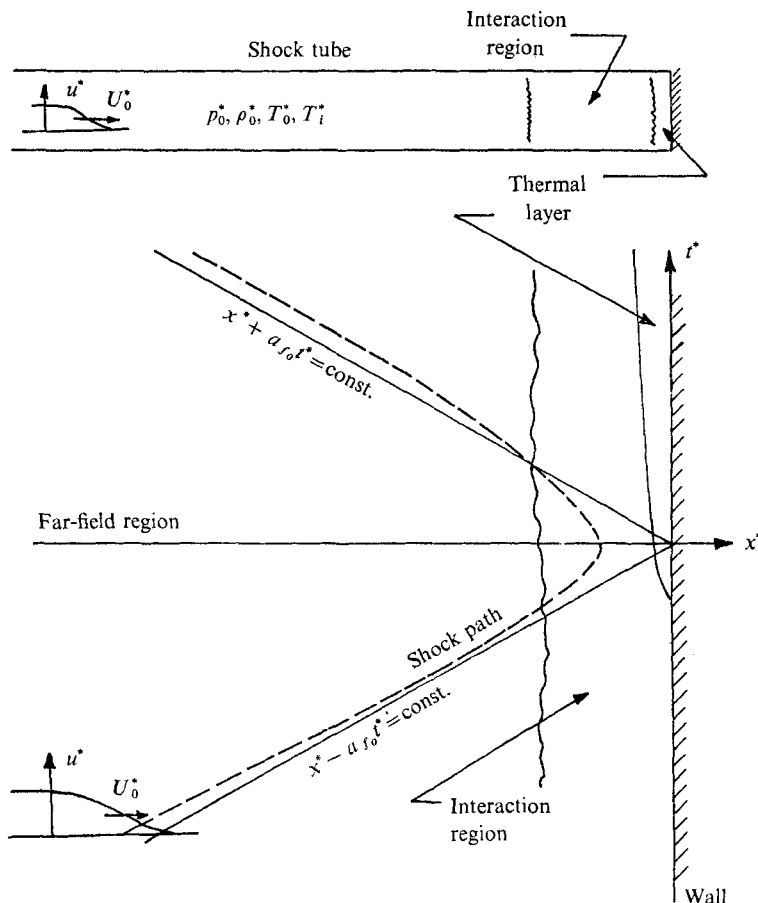


FIGURE 1. Sketch of shock tube and co-ordinate systems.

state of the quiescent gas between the shock wave and the wall. The wall is located at  $x^* = 0$ , with the gas occupying the region  $x^* < 0$ .

A zero-velocity condition at the wall is a necessary, but not a sufficient, condition for a unique solution to the problem; we must also specify the properties of the end wall. We neglect wall accommodation effects, and consider the wall to be either adiabatic or isothermal. For an adiabatic or insulated wall, there is no thermal layer adjacent to the wall, and the inner solution automatically satisfies the adiabatic wall condition. In practice the shock-tube end wall is a good conductor, and heat conduction to the wall must be considered; we make the approximation that the end wall is isothermal. End-wall heat conduction creates a very thin thermal layer that takes heat from the adjacent hotter gas and effectively attenuates the strength of the reflected shock wave. Because the thermal layer is thin, the adiabatic-wall problem is treated first, and is considered as the outer solution for treating the isothermal-wall problem. The contribution to the heat flux due to the internal temperature is taken to be small, to simplify the analysis. (For the weak shocks considered here, this imposes a restriction on the allowable difference between the frozen and equilibrium values of the

ratio of specific heats.) Thus, an adiabatic wall temperature implies  $T_{x^*}^*(0, t^*) = 0$ , and an isothermal wall requires  $T^*(0, t^*) = \text{constant}$ .

We consider a gas in which the internal energy per unit mass  $e$  is characterized by the translational and rotational temperature  $T^*$ , and the internal temperature  $T_i^*$ , by means of

$$e = c_{v_f} T^* + c_i T_i^*. \quad (2.1)$$

Here  $c_{v_f}$  and  $c_i$  are the specific heats of frozen and relaxing modes; they are assumed constant in the temperature range under consideration. We assume that  $T^*$  still satisfies the perfect-gas law  $p^* = \rho^* R T^*$ , and that the approach of the internal temperature  $T_i^*$  to the equilibrium value  $T^*$  is described by the linearized rate equation

$$\frac{DT_i^*}{Dt^*} = \frac{T^* - T_i^*}{\tau}, \quad (2.2)$$

in which  $\tau$  is the 'relaxation time' and  $D/Dt^*$  is the substantial derivative. In general,  $\tau$  is a function† of  $T^*$ ,  $p^*$  and  $T_i^*$ . Because the disturbance is weak and the departure from equilibrium is small,  $\tau$  may be treated as a constant without affecting any first- or second-order results.

In addition to (2.1) and (2.2), the equations governing unsteady one-dimensional flow of a relaxing gas are the conservation of mass, momentum, and energy, and the thermodynamic equation of state. These equations are the same as those for an equilibrium gas. The elimination of  $e$ ,  $T^*$ ,  $T_i^*$  from the governing equations (except for the heat conduction terms) leads to

$$\begin{aligned} \left(1 + \tau^* \frac{D}{Dt^*}\right) \left[ \frac{1}{\rho^*} \left( \frac{Dp^*}{Dt^*} - a_f^2 \frac{D\rho^*}{Dt^*} \right) - \frac{\gamma_f - 1}{\rho^*} k_0 \frac{\partial^2 T^*}{\partial x^{*2}} - \frac{\gamma_f - 1}{\rho^*} \left( \frac{4}{3} \mu_0 + \mu_{v_0} \right) \left( \frac{\partial u^*}{\partial x^*} \right)^2 \right] \\ = (\gamma_f - \gamma_e) \left[ \frac{p^*}{\rho^*} \frac{\partial u^*}{\partial x^*} - \frac{k_0}{\rho^*} \frac{\partial^2 T^*}{\partial x^{*2}} - \frac{1}{\rho^*} \left( \frac{4}{3} \mu_0 + \mu_{v_0} \right) \left( \frac{\partial u^*}{\partial x^*} \right)^2 \right], \end{aligned} \quad (2.3)$$

in which

$$\begin{aligned} \tau^* &= \tau(\gamma_e - 1)/(\gamma_f - 1), \quad \gamma_f = 1 + R/c_{v_f}, \\ \gamma_e &= 1 + R/c_{v_e} = 1 + R/(c_{v_f} + c_i), \end{aligned}$$

and where  $\mu_0$  is the equilibrium value of the viscosity,  $\mu_{v_0}$  that of the bulk viscosity and  $k_0$  that of the thermal conductivity; all three of these quantities are taken to be constant throughout the flow field, as their variations cause effects of higher order than those considered. We retain the viscosity and heat conduction for the moment; in the absence of end-wall heat conduction, they are of higher order, and an inviscid theory is appropriate. The coefficient  $(\gamma_f - \gamma_e)$  on the right-hand side of (2.3) determines a new parameter that measures the small departure from equilibrium. Equation (2.3) proves convenient for our problem. Using this equation, along with conservation of mass and momentum and the equation of state, we are able to avoid dealing with the non-equilibrium variable  $T_i^*$ , which can be determined from (2.2) if  $u^*$  and  $T^*$  are known. Hereafter we concentrate on determining the fluid properties  $u^*$ ,  $p^*$ ,  $\rho^*$  and  $T^*$ .

† Gunn's (1946) representation for  $\tau$  is

$$\tau^{-1} = A p^* T^{*-1} \exp[-B T^{*-1/2}] [1 - \exp(-\theta T^{*-1})],$$

where  $A$  and  $B$  are constants and  $\theta$  is the characteristic temperature of vibration.

To determine the small perturbation equations for the incoming shock wave, it is convenient to replace the physical co-ordinates  $(x^*, t^*)$  by the non-dimensional independent variables  $\xi, \bar{t}$ ,

$$\xi = \frac{1}{a_{f0}\tau^*} (x^* - a_{f0}t^*), \quad \bar{t} = \frac{\epsilon t^*}{\tau^*},$$

and define non-dimensional small-perturbation variables  $\bar{u}, \bar{p}, \bar{\rho}, \bar{T}$  by

$$u^* = a_{f0}\epsilon\bar{u}, \quad p^* = p_0^*(1 + \gamma_f\epsilon\bar{p}), \\ \rho^* = \rho_0^*(1 + \epsilon\bar{\rho}), \quad T^* = T_0^*(1 + \epsilon\bar{T}).$$

The dependent variables have asymptotic expansions of the form

$$\bar{u} = \bar{u}^{(1)} + \epsilon\bar{u}^{(2)} + \dots;$$

substituting these expansions into the governing equations, and retaining only the first-order terms in the three small parameters defined after (2.4), we find  $\bar{p}^{(1)} = \bar{\rho}^{(1)} = \bar{T}^{(1)}/(\gamma_f - 1) = \bar{u}^{(1)}$  and

$$\left(1 - \frac{\partial}{\partial \xi}\right) \left[ \frac{\partial \bar{u}^{(1)}}{\partial \bar{t}} + \frac{\gamma_f + 1}{2} \bar{u}^{(1)} \frac{\partial \bar{u}^{(1)}}{\partial \xi} - \frac{\lambda_f}{2} \frac{\partial^2 \bar{u}^{(1)}}{\partial \xi^2} \right] - \kappa \frac{\partial \bar{u}^{(1)}}{\partial \xi} = 0, \quad (2.4)$$

where  $\kappa \equiv \delta/\epsilon = (\gamma_f - \gamma_e)/2\epsilon$  is the ratio of departure from equilibrium to the shock strength and

$$\lambda_f = (1 + (\gamma_f - 1)/Pr)/\epsilon R_{a_{f0}\tau^*}.$$

Here

$$R_{a_{f0}\tau^*} = \rho_0^* a_{f0}^2 \tau^* / (\frac{4}{3}\mu_0 + \mu_{v_0})$$

is the Reynolds number based on the relaxation length scale  $a_{f0}\tau^*$  and

$$Pr = (4\mu_0/3 + \mu_{v_0})\gamma_f c_{vf}/k_0$$

is the Prandtl number. The quantity  $R_{a_{f0}\tau^*}$  is a measure of the number of collisions required for the gas to return to thermodynamic equilibrium, typically  $10^4$  or larger (the quantity  $Pr$  is typically about  $\frac{3}{2}$ ).

Equation (2.4) contains three small parameters:  $\epsilon$ ,  $R_{a_{f0}\tau^*}^{-1}$ , and  $\delta \equiv (\gamma_f - \gamma_e)/2\gamma_f$ , related to the shock strength, the ratio of viscous to inertia forces, and the departure from equilibrium. If we retain cumulative second-order terms, such as  $\epsilon\gamma_f\bar{p}^{(1)}\bar{u}_\xi^{(1)}$ , viscous effects, and approximate  $(\gamma_f - \gamma_e)/2\gamma_f$  as  $(a_{f0} - a_{e0})/a_{f0}$  and  $\gamma_f c_{vf}$  as  $\gamma_e c_{ve}$ , then (2.4) becomes (in dimensional co-ordinates)

$$\tau^* \frac{\partial}{\partial t^*} \left[ \frac{\partial \bar{u}^{(1)}}{\partial t^*} + a_{f0} \left( 1 + \frac{\gamma_f + 1}{2} \epsilon \bar{u}^{(1)} \right) \frac{\partial \bar{u}^{(1)}}{\partial x^*} - \frac{1}{\rho_0^*} \left( \frac{4}{3}\mu_0 + \mu_{v_0} + \frac{\gamma_f - 1}{\gamma_f c_{vf}} k_0 \right) \frac{\partial^2 \bar{u}^{(1)}}{\partial x^{*2}} \right] \\ + \left[ \frac{\partial \bar{u}^{(1)}}{\partial t^*} + a_{e0} \left( 1 + \frac{\gamma_e + 1}{2} \epsilon \bar{u}^{(1)} \right) \frac{\partial \bar{u}^{(1)}}{\partial x^*} - \frac{1}{\rho_0^*} \left( \frac{4}{3}\mu_0 + \mu_{v_0} + \frac{\gamma_e - 1}{\gamma_e c_{ve}} k_0 \right) \frac{\partial^2 \bar{u}^{(1)}}{\partial x^{*2}} \right] = 0,$$

which is analogous to Burgers' equation for equilibrium flows; therefore we call it the 'non-equilibrium Burgers equation'. The inviscid version of this equation was first derived by Blythe (1969). Later, (2.4) was derived by Ockendon & Spence (1969). Equation (2.4) is important for the study of unsteady non-equilibrium shock-wave structure.

Our interest is in the effect of vibrational relaxation on the shock-wave reflexion process; we simplify the problem by assuming that viscous and heat-conduction effects are negligible outside the wall thermal layer:

$$\left(1 - \frac{\partial}{\partial \xi}\right) \left(\frac{\partial \bar{u}^{(1)}}{\partial \bar{t}} + \frac{\gamma_f + 1}{2} \bar{u}^{(1)} \frac{\partial \bar{u}^{(1)}}{\partial \xi}\right) - \kappa \frac{\partial \bar{u}^{(1)}}{\partial \xi} = 0. \quad (2.5)$$

Here  $\kappa$  is the parameter whose magnitude determines whether the shock wave is fully or partly dispersed. When  $\kappa$  is large, relaxation effects are strong and the convective steepening is balanced by relaxational diffusion and the shock wave will have a continuous structure. On the other hand, when  $\kappa$  is small, relaxation effects are weak and compressions will steepen to become discontinuities with vibrational effects limited to the flow behind the shock.

Although the general analytic solution to (2.5) for arbitrary initial conditions is not readily found, (2.5) possesses a self-preserving solution and the steady-state structure can be deduced by introducing a single co-ordinate  $y = \xi - \beta \bar{t}$ , where the perturbations are functions of  $y$  alone; that is  $\bar{u}^{(1)} = \bar{u}^{(1)}(y)$ , etc., with the boundary conditions  $\bar{u}^{(1)} = 0$  or  $1$  and  $d\bar{u}^{(1)}/dy = 0$  as  $y \rightarrow \pm \infty$ . The steady-state wave speed  $U_0^*$  is equal to  $a_{f_0}(1 + \epsilon\beta)$ , where  $\beta$  is determined by boundary conditions. By writing (2.5) in terms of this shock co-ordinate,  $y$ , integrating twice and applying the boundary conditions, one deduces that

$$\beta = (\gamma_f - 1)/4 - \kappa \quad \text{or} \quad M_{f_0} \equiv U_0^*/a_{f_0} = 1 + (\gamma_f + 1) U_0^*/4a_{f_0} - (\gamma_f - \gamma_e)/2\gamma_f,$$

where  $M_{f_0}$  is the frozen Mach number.

The steady-state solutions divide into two different cases, depending upon the magnitude of the ratio of departure from equilibrium to the shock strength  $\kappa$  or upon the frozen Mach number  $M_{f_0}$ . For  $M_{f_0} < 1$  or  $\kappa > \frac{1}{4}(\gamma_f + 1)$ , the solution may be written as  $\bar{u}^{(1)} = f_1(y)$ , where  $f_1(y)$  satisfies

$$\frac{1 - f_1}{f_1^{\alpha_1}} = c_1 \exp\left(\frac{y}{2(1 - A)}\right), \quad (2.6)$$

with  $A = 2\beta/(\gamma_f + 1)$ ,  $\alpha_1 = -A(1 - A) > 0$ , and  $c_1$  an arbitrary constant related to shock-wave position. For convenience, set  $f_1 = \frac{1}{2}$  at  $y = 0$ ; then  $c_1 = (\frac{1}{2})^{\alpha_1}$ . This structure, described by Broer (1951) and Lighthill (1956), is a 'fully dispersed shock wave', and propagates at a speed intermediate between the frozen and equilibrium sound speeds. The velocity increases continuously from its initial rest equilibrium state to the final perturbation equilibrium state. For  $M_{f_0} > 1$  or  $\kappa < \frac{1}{4}(\gamma_f + 1)$ , the velocity profile given by (2.6) does not represent a continuous function; rather, it is necessary to insert a Rankine-Hugoniot shock at the wave front. The proper representation may be written as  $\bar{u}^{(1)} = 0$  for  $y > 0$ , and  $\bar{u}^{(1)} = f_2(y)$  for  $y \leq 0$ , where  $f_2(y)$  is defined by

$$(1 - f_2)f_2^{\alpha_2} = c_2 \exp\left(\frac{y}{2(1 - A)}\right), \quad (2.7)$$

with  $\alpha_2 = A/(1 - A) > 0$ , and  $c_2$  determined from the Rankine-Hugoniot conditions with the vibrational mode frozen through the shock front. In our notation, the velocity jumps from the value  $\bar{u}^{(1)} = 0$  to  $f_s$ , where

$$f_s = (\gamma_f + 1)(M_{f_0}^2 - 1)/2\epsilon M_{f_0} \quad \text{at} \quad y = 0 \quad \text{and} \quad c_2 = (1 - f_s)f_s^{\alpha_2}.$$

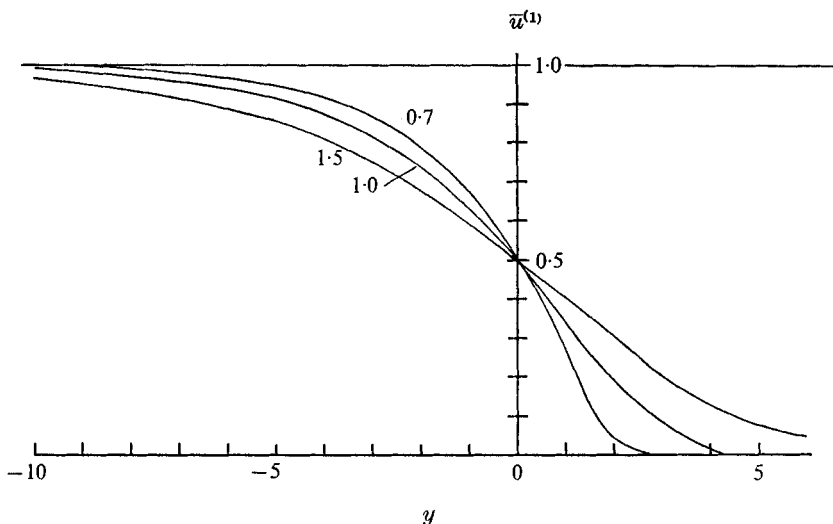


FIGURE 2. The steady-state velocity profile of fully dispersed shock waves, varying  $\kappa = (\gamma_f - \gamma_e)/2\epsilon\gamma_f$ . (Curves labelled with values of  $\kappa$ .)

This partly dispersed shock wave propagates at a speed greater than the frozen sound speed. The wave consists of a Rankine-Hugoniot shock followed by a gradual further compression which extends over the ‘relaxation zone’. Thus, we have assumed that the translational and rotational modes adjust to new equilibrium values instantaneously across the Rankine-Hugoniot shock, and that the vibrational energy is frozen during this stage. In the relaxation region, the vibrational temperature adjusts gradually to its equilibrium value, while the translational and rotational modes remain in local equilibrium.

The remaining independent variables  $\bar{\rho}^{(1)}$ ,  $\bar{p}^{(1)}$  and  $\bar{T}^{(1)}$  are related by

$$\bar{p}^{(1)} = \bar{\rho}^{(1)} = \bar{T}^{(1)}/(\gamma_f - 1)$$

and equal to  $f_1(y)$  if  $M_{f0} < 1$ , or equal to  $f_2(y)$ , if  $M_{f0} > 1$ . Substitution into the rate equation (2.2) determines  $T_i^*$ :  $T_i^* = T_0^*(1 + \epsilon\bar{T}_i^{(1)})$ , where

$$\bar{T}_i^{(1)} = \begin{cases} \frac{(\gamma_e - 1)}{(\gamma_f - 1)^2} \exp\left(\frac{\gamma_e - 1}{\gamma_f - 1} y\right) \int_{\infty}^y f_1(\xi) \exp\left(-\frac{\gamma_e - 1}{\gamma_f - 1} \xi\right) d\xi & \text{for } M_{f0} < 1, \\ \left. \begin{aligned} &\frac{(\gamma_e - 1)}{(\gamma_f - 1)^2} \exp\left(\frac{\gamma_e - 1}{\gamma_f - 1} y\right) \int_0^y f_2(\xi) \exp\left(-\frac{\gamma_e - 1}{\gamma_f - 1} \xi\right) d\xi & (y \leq 0) \\ &0 & (y > 0) \end{aligned} \right\} & \text{for } M_{f0} > 1. \end{cases}$$

For  $M_{f0} < 1$  there is a gradual increase of temperature and vibrational energy through the whole wave, and for  $M_{f0} > 1$ , following the Rankine-Hugoniot jump, there also is a gradual increase of temperature in the relaxation zone. This is quite different from the strong shock wave case, where the temperature decreases behind the Rankine-Hugoniot shock wave as the vibrational mode becomes excited. For intermediate shock strengths the behaviour is more complex (see Bethe & Teller 1941). Becker (1970) has sketched the velocity and



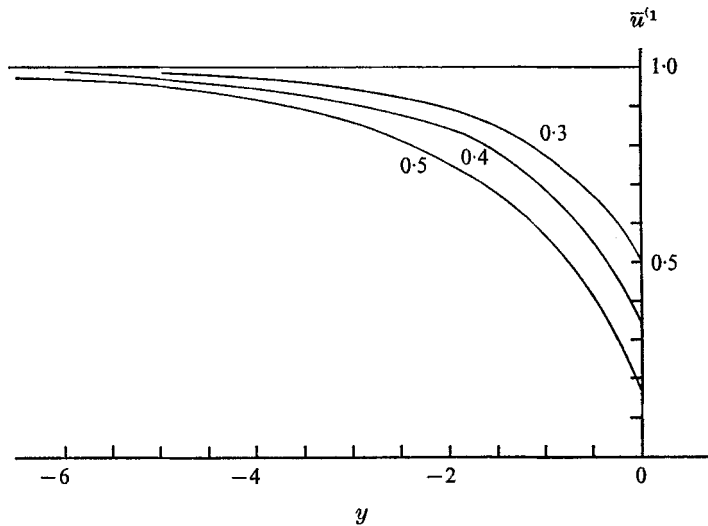


FIGURE 3. The steady-state velocity profile of partly dispersed shock waves, varying  $\kappa = (\gamma_f - \gamma_e)/2\epsilon\gamma_f$  ( $\epsilon = 0.01$ ). (Curves labelled with values of  $\kappa$ .)

temperature profiles for increasing shock strengths for two different values of  $\gamma_f/\gamma_e$ .

Figures 2 and 3 display the steady-state solutions of fully and partly dispersed shock waves, for moderate  $\kappa$ 's. There are three limiting cases. For  $\kappa$  very large, the relaxation zone becomes very long, and the velocity profile is almost constant over the relaxation length scale  $a_{f0}\tau^*$ . For  $\kappa$  very small,

$$M_{f0} \rightarrow 1 + (\gamma_f + 1)u_0^*/4a_{f0}^*,$$

and the velocity profile is represented by a step function that has the same jump as an equilibrium shock wave followed by a 'vibrational tail'. For  $\kappa \rightarrow \frac{1}{4}(\gamma_f + 1)$ , the frozen Mach number  $M_{f0} \rightarrow 1$  and the velocity profile is approximately zero for  $y > 0$  and

$$\bar{u}^{(1)} = [1 - (1 - 2A)\exp(\frac{1}{2}y/(1 - A))] \quad \text{for } y \leq 0,$$

which is a simple exponential behaviour. The behaviour depicted in figures 2 and 3 is most easily interpreted by considering conditions intermediate to these limiting cases.

### 3. Shock reflexion from an adiabatic wall

As a fully dispersed shock wave nears the wall it begins to interact with the wall. For a partly dispersed wave, which propagates slightly faster than the undisturbed frozen sound speed, there is no interaction with the wall until it reaches the wall. After reflecting from the end wall, the waves propagate through a time-varying relaxation zone which is a part of the incident wave. From the far-field solution we know that the thickness of the relaxation region is  $O(a_{f0}\tau^*)$  and that the shock speed is near  $a_{f0}$ ; therefore, the interaction of incident and

reflected waves occurs on a characteristic time scale of order  $\tau^*$ . Hence, the interaction inner region is delineated by  $x^* = O(a_{f0}\tau^*)$  and  $t^* = O(\tau^*)$ . In this short time and spatial interval, it is reasonable to anticipate that convection terms, which vanish at the wall, are of higher order, and that to lowest order the phenomenon of shock-wave reflexion is governed by a linear equation. To observe the details of reflexion, we introduce dimensionless independent variables

$$x = \frac{x^*}{a_{f0}\tau^*}, \quad t = \frac{t^*}{\tau^*},$$

and define the non-dimensional perturbed dependent variables, as in the far-field region, to be  $u$ ,  $p$ ,  $\rho$  and  $T$ . Again we expand the dependent variables in a power series in  $\epsilon$ , and then find that the first-order approximation for the velocity satisfies

$$\left(1 + \frac{\partial}{\partial t}\right) \left(\frac{\partial^2 u^{(1)}}{\partial t^2} - \frac{\partial^2 u^{(1)}}{\partial x^2}\right) = 0. \quad (3.1)$$

The other first-order quantities, such as temperature, pressure and density, also satisfy this equation. If the term  $(\gamma_f - \gamma_e)u_x^{(1)}/\gamma_f$ , which is  $O(\delta)$ , is retained in the derivation, (3.1) can be rewritten in dimensional co-ordinates  $(x^*, t^*)$  as

$$\tau^* \frac{\partial}{\partial t^*} \left(\frac{\partial^2 u^{(1)}}{\partial t^{*2}} - a_{f0}^2 \frac{\partial^2 u^{(1)}}{\partial x^{*2}}\right) + \left(\frac{\partial^2 u^{(1)}}{\partial t^{*2}} - a_{e0}^2 \frac{\partial^2 u^{(1)}}{\partial x^{*2}}\right) = 0, \quad (3.2)$$

which is usually derived on the basis of the acoustic approximation and is appropriate for the case  $(a_{f0} - a_{e0})/a_{f0} = O(1)$ . Equation (3.2) has been employed by many authors to study the non-equilibrium problems, and the character of the solution is well known. At times small compared with  $\tau^*$ , the higher-order operator associated with frozen speed controls the propagation of disturbances; but, at large times, it is the equilibrium sound speed which governs the motion. Equation (3.1) is simpler; there is only one speed controlling the motion since the equilibrium speed is approximated by the frozen sound speed.

The boundary condition for shock-wave reflexion is zero velocity at the wall. The initial conditions are imposed by requiring the solution to approach the incoming steady-state solution as  $t \rightarrow -\infty$ . We first examine the fully dispersed wave, then proceed by analogy with the partly dispersed case.

### 3.1. Fully dispersed shock wave

If  $M_{f0} < 1$ , the structure of the wave is everywhere differentiable any number of times. As an initial condition we require that  $u(x, t; \epsilon)$  approach the far-field solution written in inner co-ordinates  $(x, t)$ ; i.e. as  $t \rightarrow -\infty$ ,  $u(x, t) \rightarrow f_1(x - t - \epsilon\beta t)$ , where the function  $f_1$  is defined by (2.6). With  $\epsilon \rightarrow 0$ , we find that, as  $x, t \rightarrow -\infty$ ,  $u^{(1)}(x, t) \rightarrow f_1(x - t)$  provides the matching condition for the first-order solution. To solve (3.1), we split the equation into

$$\frac{\partial^2 u^{(1)}}{\partial t^2} - \frac{\partial^2 u^{(1)}}{\partial x^2} = F(x, t) \quad \text{and} \quad \frac{\partial F}{\partial t} + F = 0,$$

such that both equations have simple general solutions. The only solution for the second equation that has  $F(x, t)$  bounded for  $t \rightarrow -\infty$  is  $F(x, t) = 0$ , and the

first equation reduces to the wave equation. Applying the boundary condition and matching with the far-field solution, we find  $u^{(1)}(x, t) = f_1(x, t) - f_1(x - t)$ . The remaining first-order approximate variables are

$$p^{(1)} = \rho^{(1)} = T^{(1)} / (\gamma_f - 1) = f_1(x - t) + f_1(-x - t).$$

This shows that the first-order asymptotic solution in this region is only a superposition of left- and right-going waves of equal strength, in which the gas velocities cancel at the wall, and other thermodynamic properties, such as pressure, density and temperature, are additive there. This is classical acoustic reflexion.

To investigate the convective and dispersive effects in this inner region, we must use the second-order approximation. The equations governing the second-order terms are found by substituting the asymptotic power series into the governing equations, and using the first-order results. Thus, we find the second-order equations

$$\left. \begin{aligned} \rho_t^{(2)} + u_x^{(2)} &= -(\rho^{(1)}u^{(1)})_x, \\ u_t^{(2)} + p_x^{(2)} &= -(\rho^{(1)}u_t^{(1)} + u^{(1)}u_x^{(1)}), \\ \gamma_f p^{(2)} - \rho^{(2)} - T^{(2)} &= \rho^{(1)}T^{(1)}, \end{aligned} \right\} \quad (3.3)$$

and

$$\left(1 + \frac{\partial}{\partial t}\right)(u_{tt}^{(2)} - u_{xx}^{(2)}) = \left(1 + \frac{\partial}{\partial t}\right)[\rho^{(1)}u_{tt}^{(1)} + u^{(1)}u_{xt}^{(1)} - (u^{(1)}p_x^{(1)} + \gamma_f p^{(1)}u_x^{(1)})_x] - 2\kappa u_{xx}^{(1)}. \quad (3.4)$$

Equation (3.4) is a non-homogeneous wave equation, analogous to a non-homogeneous classical wave equation for the second-order approximation in gas-dynamics. With  $u^{(2)}(x, t)$  determined by (3.4), the relations (3.3) prescribe the second-order density, pressure and temperature. Equations (3.3) and (3.4) are valid ahead of, and behind, the discontinuity for the case of a partly dispersed shock wave. A judicious interpretation of the expansion  $u^{(1)} + \epsilon u^{(2)}$  is necessary to get the correct speed for the discontinuity.

Variations in the relaxation time  $\tau^*$  do not affect the result to this order. For, if we write  $\tau^* = \tau_0^*(1 + \epsilon\tau^{(1)})$ , the effect of the term  $\epsilon\tau^{(1)}$  is second order, and appears in the right-hand side of (3.4) as  $\tau^{(1)}(u_{tt}^{(1)} - u_{xx}^{(1)})_t$ , which is zero.

It is convenient to write (3.4) in terms of characteristic co-ordinates  $\xi = x - t$  and  $\eta = x + t$ , which we shall use interchangeably with  $(x, t)$  in the interaction region; they should not be confused with the  $(\xi, \bar{t})$  or  $(\eta, \bar{t})$  co-ordinate systems in the far-field regions. Substituting for  $u^{(1)}, \rho^{(1)}, p^{(1)}$ , we find

$$u_t^{(2)} + u^{(2)} = F^{(2)}(x, t), \quad (3.5)$$

$$\begin{aligned} 4F_{\xi\eta}^{(2)} &= [-(1 + \gamma_f)f_1'(\xi)f_1(\xi) + 2\kappa f_1'(\xi) + (3 - \gamma_f)f_1'(\xi)f_1(-\eta)]_{\xi} \\ &+ [-(1 + \gamma_f)f_1'(-\eta)f_1(-\eta) + 2\kappa f_1'(-\eta) + (3 - \gamma_f)f_1'(-\eta)f_1(\xi)]_{\eta} \\ &+ [(\gamma_f + 1)f_1''(\xi)f(\xi) + (\gamma_f + 1)f_1'^2(\xi) - (3 - \gamma_f)f_1''(\xi)f_1(-\eta)]_{\xi} \\ &+ [(\gamma_f + 1)f_1''(-\eta)f_1(-\eta) + (\gamma_f + 1)f_1'^2(-\eta) - (3 - \gamma_f)f_1''(-\eta)f_1(\xi)]_{\eta} \\ &+ (3 - \gamma_f)[f_1'(\xi)f_1(-\eta) - f_1'(-\eta)f_1(\xi)]_{\xi\eta}, \end{aligned} \quad (3.6)$$

where the prime denotes differentiation with respect to the function's argument.

The boundary conditions required for the zero-velocity wall condition are that  $u^{(2)}(0, t) = 0$ , and so  $w_t^{(2)}(0, t) = 0$ ; this implies  $F^{(2)}(0, t) = 0$  for (3.6). Initial conditions are supplied by the asymptotic matching principle of Van Dyke (1964): match the one-term far-field with the two-term inner expansion; that is, the two-term inner co-ordinate representation of the two-term outer far-field solution is set equal to the one-term far-field co-ordinate representation of the two-term inner solution. Thus, we find that, as  $t \rightarrow -\infty$  with  $x-t$  fixed,

$$u^{(2)}(x, t) \rightarrow -\beta t f_1'(x-t);$$

so

$$F^{(2)}(\xi, \eta) \rightarrow -\beta [t f_1'(\xi) - t f_1''(\xi) + f_1'(\xi)].$$

Integrating (3.6) twice, and satisfying the above matching condition, we find  $F^{(2)}(x, t)$ ; solving the first-order non-homogeneous linear partial differential equation (3.5) with the initial condition is then a straightforward, albeit lengthy, task. The final result for the second-order velocity is found to be

$$u^{(2)} = -\beta t (f_1'(x-t) - f_1'(-x-t)) \\ - \frac{3-\gamma_f}{4} (f_1'(x-t) \Phi_1(-x-t) - f_1'(-x-t) \Phi_1(x-t)),$$

where  $\Phi_1(\xi) = 2(1-A) [(1-\alpha_1)f_1(\xi) + \log(1-f_1(\xi))].$

Substituting the second-order velocity  $u^{(2)}$  into the first two equations of (3.3), and integrating with respect to  $x$  and  $t$ , respectively, we find that

$$\rho^{(2)} = -\beta t (f_1'(\xi) + f_1'(-\eta)) - \beta (f_1(\xi) + f_1(-\eta)) + f_1^2(\xi) + f_1^2(-\eta) \\ - \frac{3-\gamma_f}{4} (f_1'(\xi) \Phi_1(-\eta) + f_1'(-\eta) \Phi_1(\xi) - 2f_1(\xi)f_1(-\eta)), \\ p^{(2)} = -\beta t (f_1'(\xi) + f_1'(-\eta)) + \beta (f_1(\xi) + f_1(-\eta)) + 2f_1(\xi)f_1(-\eta) \\ - \frac{3-\gamma_f}{4} (f_1'(\xi) \Phi_1(-\eta) + f_1'(-\eta) \Phi_1(\xi) + 2f_1(\xi)f_1(-\eta)).$$

With the second-order solutions for density and pressure known, the temperature  $T^{(2)}$  can be evaluated by using the third equation of (3.3). We note that, as  $t \rightarrow -\infty$  with  $x-t$  fixed, the combination of first- and second-order solutions for pressure, written in the far-field representation, is  $p^{(1)} + \epsilon p^{(2)} \rightarrow f_1(\xi) - \beta t f_1'(\xi) + \epsilon \beta f_1(\xi)$ , which matches the first-order far-field solutions except for the second-order term  $\epsilon \beta f_1(\xi)$ . This occurs for density and temperature as well, and may be remedied by carrying out the second-order far-field expansion. As we need  $u$  only to second order, this is not undertaken here.

### 3.2. Partly dispersed shock wave

For a partly dispersed shock wave there is no interaction with the wall until the wave front reaches it. After reflexion from the wall, the discontinuous jump propagates through the relaxation zone that has followed it to the wall. The velocity profile  $f_2$ , given by (2.7), is complicated, and it is impossible to find an analytical relation predicting the precise strength of the reflected Rankine-Hugoniot shock at any instant  $t$ . As (3.1) and (3.4) both possess two constant-

speed wave operators (with different signs), it is reasonable for us to expect that the reflected shock front propagates through the relaxation zone at constant speed. We proceed with this approximation (as did Hanson 1971 *a*), which is clearly justified in a first-order approximation, and avoids the difficulty of finding the jump condition at any instant. While the procedure is not locally correct to second order, it does give the correct asymptotic speed for the discontinuity with the proper interpretation of  $w^{(1)} + \epsilon w^{(2)}$ . As we need this result, we report it noting that it is only correct to first order locally. We generalize the definition of the function  $f_2(y)$  as follows. For  $y > 0$ ,  $f_2 = 0$ , and for  $y \leq 0$ ,  $f_2(y)$  satisfies the relation (2.7); hence the far-field, incident, partly dispersed shock wave is given by  $\bar{w}^{(1)}(y) = f_2(y)$  for  $-\infty < y < \infty$ . By considering the left and right derivatives for  $f_2$  as  $y \rightarrow 0$ , we may treat  $f_2(y)$  as a single-valued function that is everywhere thrice differentiable. Hence, the calculation for the reflexion of a partly dispersed shock wave, which involves third derivatives, is essentially the same as that for a fully dispersed shock, except that we insert the Rankine-Hugoniot relations for the shock-front jump conditions.

Following the procedure employed to solve the fully dispersed case, we find the first- and second-order velocity to be

$$w^{(1)} = f_2(\xi) - f_2(-\eta),$$

$$\text{and } w^{(2)} = -\beta t [f_2'(\xi) - f_2'(-\eta)] - \frac{3-\gamma_f}{4} [f_2'(\xi) \Phi_2(-\eta) - f_2'(-\eta) \Phi_2(\xi)],$$

$$\text{where } \Phi_2 = 2(1-A) [(1 + \alpha_2) f_2(\xi) + \log(1 - f_2(\xi))].$$

Similar expressions for density, pressure and temperature can also be found. For  $t < 0$  (i.e.  $\eta < 0$ ), the terms including functions of  $\eta$  are zero, and there is no contribution, so that there is no reflexion and no interaction. The Rankine-Hugoniot shock front reaches the end wall  $x = 0$  at  $t = 0$ , and is then reflected from the wall, propagating through the time-varying relaxation zone behind the incident shock with a speed that is initially approximated by the frozen sound speed  $a_{f0}$ , and, as we shall see, approaches the speed  $a_{f0}(1 - \kappa + \frac{1}{4}(5 - 3\gamma_f))$  as it leaves the interaction region.

This completes the interaction (inner) solutions for both the fully and partly dispersed waves. It is to be noted that, at the end wall, the first-order solutions for temperature, pressure, and density are non-decreasing functions with respect to time  $t$ . But their gradients with respect to space, viz.  $T_x^{(1)}$ ,  $p_x^{(1)}$ ,  $\rho_x^{(1)}$ , all vanish at  $x = 0$ . Moreover, even the first derivatives with respect to  $x$  of the second-order solutions for these variables vanish at the wall. This implies that the temperature, pressure and density have extreme values at the wall. This is consistent with the adiabatic wall condition for a heat-conducting gas, which requires that

$$T_x^{(1)}(0, t) = T_x^{(2)}(0, t) = 0.$$

These inner solutions will not be valid for large times after reflexion; the solutions for the second-order approximations contain secular terms such as  $tf'(x-t)$ , where  $f'$  denotes  $f_1'$  for the fully dispersed shock wave and  $f_2'$  for the partly dispersed wave. Consequently, for  $t = O(\epsilon^{-1})$ , the inner asymptotic

expansion for velocity becomes invalid. For  $t \rightarrow -\infty$ , these solutions match with the incident far-field solution. To obtain a valid expansion for  $t \rightarrow +\infty$ , we need the left-going version of the far-field wave equation. Written in co-ordinates analogous to (2.5)

$$\eta = \frac{1}{af_0\tau^*} (x^* + a_{f0}t^*), \quad \bar{t} = \frac{\epsilon t^*}{\tau^*},$$

the first-order result is obviously

$$\left(1 + \frac{\partial}{\partial \eta}\right) \left[ \frac{\partial \bar{u}^{(1)}}{\partial \bar{t}} + \left(\frac{\gamma_f + 1}{2} \bar{u}^{(1)} - \gamma_f + 1\right) \frac{\partial \bar{u}^{(1)}}{\partial \eta} \right] + \kappa \frac{\partial \bar{u}^{(1)}}{\partial \eta} = 0, \tag{3.7}$$

with the auxiliary relation

$$\bar{p}^{(1)} = \bar{\rho}^{(1)} = \bar{T}^{(1)} / (\gamma_f - 1) = 2 - \bar{u}^{(1)}(\eta, \bar{t})$$

and with the boundary conditions  $\bar{u} \rightarrow 1$  as  $\eta \rightarrow -\infty$  and  $\bar{u} \rightarrow 0$  as  $\eta \rightarrow +\infty$ .

By analogy with our matching of the incident shock wave with the interaction region solution, one can see that the first-order matching condition is equivalent to the requirement that, as  $\bar{t} \rightarrow 0^+$ ,  $\bar{u}^{(1)}(\eta, \bar{t}) \rightarrow 1 - f_{1,2}(-\eta) + O(\epsilon)$ . If we compare the matching conditions above with the steady-state solution of (3.7), we can conclude that the appropriate solutions are

$$\bar{u}^{(1)} = 1 - f_{1,2} \left( -\eta + \left( \frac{5 - 3\gamma_f}{4} + \kappa \right) \bar{t} \right).$$

It can easily be verified that the second-order interaction solution for velocity properly matches with this solution. However, as in the case of the incident wave, the second-order interaction solutions for temperature, pressure and density cannot be matched with the first-order outgoing solutions for those quantities without additional computations.

To construct the uniformly valid composite expansion for velocity, we employ the additive-composition principle; the sum of the interaction and the far-field solution is corrected by subtracting the part they have in common. Thus the composite expansion for velocity of the fully dispersed shock is given by

$$u_{\text{comp}} = f_1 \left( \xi - \left( \frac{\gamma_f - 1}{4} - \kappa \right) \bar{t} \right) - f_1(-\eta) + \epsilon \left[ \left( \frac{\gamma_f - 1}{4} - \kappa \right) \bar{t} f_1'(-\eta) - \frac{3 - \gamma_f}{4} (f_1'(\xi) \Phi_1(-\eta) - f_1'(-\eta) \Phi_1(\xi)) \right] \tag{for } \bar{t} \leq 0,$$

and

$$u_{\text{comp}} = f_1(\xi) - f_1 \left( -\eta + \left( \frac{5 - 3\gamma_f}{4} + \kappa \right) \bar{t} \right) - \epsilon \left[ \left( \frac{\gamma_f + 1}{4} - \kappa \right) \bar{t} f_1'(\xi) - \frac{3 - \gamma_f}{2} \bar{t} f_1'(-\eta) + \frac{3 - \gamma_f}{4} (f_1'(\xi) \Phi_1(-\eta) - f_1'(-\eta) \Phi_1(\xi)) \right] \tag{for } \bar{t} > 0.$$

For the partly dispersed shock, we must determine the composite trajectory of the shock front. We write the composite trajectory, for  $\bar{t} < 0$ , as

$$\xi - \left( \frac{1}{4}(\gamma_f + 1) - \kappa \right) \bar{t} = 0 \quad \text{and, for } \bar{t} \geq 0, \quad \text{as } \eta - \left( \frac{1}{4}(5 - 3\gamma_f) + \kappa \right) \bar{t} = 0.$$

Hence, the composite expansion for velocity of the partly dispersed shock is given by

$$u_{\text{comp}} = f_2 \left( \xi - \left( \frac{\gamma_f + 1}{4} - \kappa \right) \bar{t} \right) \quad \text{for } \bar{t} < 0,$$

and

$$\begin{aligned} u_{\text{comp}} = & f_2(\xi) - f_2 \left( -\eta + \left( \frac{5 - 3\gamma_f}{4} + \kappa \right) \bar{t} \right) - \epsilon \left[ \left( \frac{\gamma_f + 1}{4} - \kappa \right) \bar{t} f_2'(\xi) \right. \\ & + \frac{3 - \gamma_f}{4} \left\{ f_2'(\xi) \Phi_2 \left( -\eta + \left( \frac{5 - 3\gamma_f}{4} + \kappa \right) \bar{t} \right) - f_2' \left( -\eta + \left( \frac{5 - 3\gamma_f}{4} + \kappa \right) \bar{t} \right) \Phi_2(\xi) \right\} \\ & \left. - \frac{3 - \gamma_f}{2} \bar{t} f_2' \left( -\eta + \left( \frac{5 - 3\gamma_f}{4} + \kappa \right) \bar{t} \right) \right] \quad \text{for } \bar{t} \geq 0. \end{aligned}$$

The uniformly valid composite representations of the density, pressure, and temperature can be formed in the same way.

#### 4. The isothermal wall

In §§2 and 3 we assumed that the viscosity and heat conductivity were negligible. Thus the zero-velocity wall condition is a sufficient boundary condition, and the temperature gradient at the wall  $T_x(0, t)$  is zero for both the first- and second-order solutions. This implies that the non-equilibrium wave equation which we derived and employed in §3 is unable to cope with an arbitrary temperature or heat-flux boundary condition. Here again, the problem is one of the singular-perturbation type and is solved by the introduction of a thermal boundary layer adjacent to the wall. We first calculate the thermal boundary layer (§4.1), then determine its effect on the interaction region (§4.2) and subsequently on the reflected shock trajectory (§4.3).

##### 4.1. The thermal boundary layer

Heat conduction to the wall is of importance only in a layer near the wall that initially is very thin. As pointed out by Goldsworthy (1959), the pressure in this thin thermal layer is independent of  $x^*$ . Thus, after an appropriate stretching, the equations governing the first-order terms in a thermal-layer expansion will indicate the absence of a pressure gradient.

The new small parameter for the thermal-layer expansion is  $\hat{\epsilon} \equiv 1/R_{af_0}^{\frac{1}{2}} \tau^*$ ; from the previous assumption that  $\epsilon R_{af_0} \tau^* \gg 1$ , we have a realistic restraint that  $\epsilon \gg \hat{\epsilon}^2$ . The appropriate thermal-layer co-ordinates  $(\hat{x}, \hat{t})$  are defined by the stretching  $\hat{x} = x/\hat{\epsilon}$  and  $\hat{t} = t$ , where  $x, t$  are dimensionless variables defined in §3. The thermal-layer dependent variables  $\hat{u}(\hat{x}, \hat{t}; \hat{\epsilon})$ ,  $\hat{p}(\hat{x}, \hat{t}; \hat{\epsilon}) \dots$ , defined by analogy with §2, are expanded in the form

$$\begin{aligned} \hat{u} &= \hat{\epsilon} \hat{u}^{(1)}(\hat{x}, \hat{t}) + \hat{\epsilon}^2 \hat{u}^{(2)}(\hat{x}, \hat{t}) + \dots, \\ \hat{p} &= \hat{p}^{(1)}(\hat{x}, \hat{t}) + \hat{\epsilon} \hat{p}^{(2)}(\hat{x}, \hat{t}) + \dots, \end{aligned}$$

etc. The variations of fluid properties in the thermal-layer region are the same order of magnitude as those in the interaction region, but the velocity is of higher order here, being  $O(\epsilon \hat{\epsilon})$ ; thus we again expect convection and dissipation to be negligible, and the governing equations to be linear.

Substitution of the thermal-layer expansions into the basic equations, expressed in the stretched co-ordinates  $(\hat{x}, \hat{t})$ , yields the set of first-order equations

$$\hat{\rho}_{\hat{t}}^{(1)} + \hat{u}_{\hat{x}}^{(1)} = 0, \quad \hat{p}_{\hat{x}}^{(1)} = 0, \quad \gamma_f \hat{p}^{(1)} = \hat{T}^{(1)} + \hat{\rho}^{(1)}, \quad (4.1)$$

and

$$\left(1 + \frac{\partial}{\partial \hat{t}}\right) \left(\hat{p}_{\hat{t}}^{(1)} + \hat{u}_{\hat{x}}^{(1)} - \frac{1}{Pr} \hat{T}_{\hat{x}\hat{x}}^{(1)}\right) = 0. \quad (4.2)$$

Equations (4.1) and (4.2) are in a form suitable for the problem with an arbitrary wall-temperature condition; the adiabatic-wall solution automatically satisfies (4.1) and (4.2).

We assume, for simplicity, that the wall is isothermal. This is a good approximation in many experimental situations. The variation of the end-wall temperature was less than 1% in the experiments of Sturtevant & Slachmuylders (1964). Thus  $\hat{T}^{(1)}(0, \hat{t}) = 0$  and  $\hat{u}^{(1)}(0, \hat{t}) = 0$ . Other boundary conditions are provided by matching the solution for this region to that for the interaction region. We treat the fully and partly dispersed shock waves separately.

4.1.1. *Fully dispersed shock wave.* The thermal-layer representation of the first-order adiabatic velocity as  $x \rightarrow 0$  is  $u^{(1)} \approx 2\hat{x}f_1'(-\hat{t})\hat{e}$ . This provides the matching condition for the thermal-layer velocity. As  $\hat{x} \rightarrow -\infty$ ,  $\hat{u}^{(1)} \rightarrow 2\hat{x}f_1'(-\hat{t})$ . Similarly, for other dependent variables, we find the matching conditions are, as  $\hat{x} \rightarrow -\infty$ ,  $\hat{p}^{(1)} = \hat{\rho}^{(1)} = \hat{T}^{(1)}/(\gamma_f - 1) \rightarrow 2f_1(-\hat{t})$ . This follows from the second equation of (4.1), which leads to a simple solution for pressure and gives the pressure history at the shock-tube end wall, and permits simplification of (4.2) to a 'non-equilibrium diffusion equation'

$$\left(1 + \frac{\partial}{\partial \hat{t}}\right) \left(\hat{T}_{\hat{t}}^{(1)} - \frac{1}{Pr} \hat{T}_{\hat{x}\hat{x}}^{(1)} + 2(\gamma_f - 1)f_1'(-\hat{t})\right) = 0,$$

or

$$\hat{T}_{\hat{t}}^{(1)} - \frac{1}{Pr} \hat{T}_{\hat{x}\hat{x}}^{(1)} + 2(\gamma_f - 1)f_1'(-\hat{t}) = c(\hat{x})e^{-\hat{t}}, \quad (4.3)$$

where  $c(\hat{x})$  is an arbitrary function. The right-hand side of (4.3) is the general solution for the operator  $(1 + \partial/\partial \hat{t})$ . Satisfying the essential condition that the solution is bounded throughout  $-\infty < \hat{t} < \infty$ , we conclude that  $c(\hat{x}) = 0$ . Now (4.3) can be solved by taking the Fourier transform with respect to time.

Satisfying the boundary and matching conditions, it follows at once that the first-order solutions for temperature, density and velocity in the thermal boundary layer are given by

$$\left. \begin{aligned} \hat{T}^{(1)} &= 2(\gamma_f - 1)f_1(-\hat{t}) + \theta_1(\hat{x}, \hat{t}), \\ \hat{\rho}^{(1)} &= 2f_1(-\hat{t}) - \theta_1(\hat{x}, \hat{t}), \end{aligned} \right\} \quad (4.4)$$

and

$$\begin{aligned} \hat{u}^{(1)} &= 2\hat{x}f_1'(-\hat{t}) + \frac{1}{Pr} \theta_{1\hat{x}} \Big|_0^{\hat{x}} \\ &= 2\hat{x}f_1'(-\hat{t}) + \frac{\gamma_f - 1}{(\pi Pr)^{\frac{1}{2}}} \int_{-\infty}^{\hat{t}} \frac{f_1(-\tau)}{(\hat{t} - \tau)^{\frac{1}{2}}} \left[ \left(1 - \frac{Pr\hat{x}^2}{2(\hat{t} - \tau)}\right) \exp\left(\frac{-Pr\hat{x}^2}{4(\hat{t} - \tau)}\right) - 1 \right] d\tau, \end{aligned}$$

where

$$\theta_1(\hat{x}, \hat{t}) = \frac{(\gamma_f - 1)Pr^{\frac{1}{2}}}{\pi^{\frac{1}{2}}} \int_{-\infty}^{\hat{t}} f_1(-\tau) \frac{\hat{x}}{(\hat{t} - \tau)^{\frac{3}{2}}} \exp\left(\frac{-Pr\hat{x}^2}{4(\hat{t} - \tau)}\right) d\tau. \quad (4.5)$$



The first terms of (4.4) and (4.5) are the adiabatic solution in the thermal-layer region; the second terms represent the influence of heat conduction. Care must be exercised in determining  $\hat{u}^{(1)}$  for  $\hat{x} \rightarrow 0$ , because the denominator appearing in the integrand of  $\theta_{1\hat{x}}$  approaches zero as  $\tau \rightarrow \hat{t}$ .

4.1.2. *Partly dispersed shock wave.* In this case, we are interested only in  $\hat{t} \geq 0$ ; for  $\hat{t} < 0$ , the gas temperature at the wall is constant and equal to  $T_0^*$ . At  $\hat{t} = 0$ , the incident shock front meets and then reflects from the end wall and all the thermodynamic properties such as temperature, pressure and density jump to values determined by Rankine–Hugoniot relations. Heat conduction, however, keeps the wall at the constant temperature  $T_0^*$ . After  $\hat{t} \gtrsim 4\gamma_f/PrR_{\alpha_f}\tau^*$ , the reflected shock front has traversed the thermal layer; consequently we assume that there is no Rankine–Hugoniot jump in the thermal-boundary-layer region. This allows us to determine the matching conditions by representing the adiabatic-wall solution in thermal-layer co-ordinates  $(\hat{x}, \hat{t})$  without worrying about the discontinuous behaviour of  $f_2(x-t)$  and  $f_2(-x-t)$ . As in the fully dispersed case, the governing equation is (4.3), but with  $f_1'(-\hat{t})$  replaced by  $f_2'(-\hat{t})$ . Here, however, we have an initial-value problem with

$$\left. \begin{aligned} \hat{T}^{(1)}(\hat{x}, 0) &= 2(\gamma_f - 1)f_2(0), \\ \hat{T}_{\hat{t}}^{(1)}(\hat{x}, 0) &= -2(\gamma_f - 1)f_2'(0) \end{aligned} \right\}$$

and

$$\hat{T}_{\hat{x}}^{(1)}(\hat{x}, 0) = \hat{T}_{\hat{x}\hat{x}}^{(1)}(\hat{x}, 0) = 0.$$

These initial conditions conform with our assumption that, at  $\hat{t} = 0$ , the reflected shock front has already reached some  $\hat{x} \gg 1$ , and has a uniform temperature field behind it. Satisfying these conditions, we again conclude that  $c(\hat{x}) = 0$ , and find

$$\left. \begin{aligned} \hat{T}^{(1)} &= 2(\gamma_f - 1)f_2(-\hat{t}) + \theta_2(\hat{x}, \hat{t}), \\ \hat{\rho}^{(1)} &= 2f_2(-\hat{t}) - \theta_2(\hat{x}, \hat{t}), \end{aligned} \right\} \quad (4.6)$$

$$\hat{u}^{(1)} = 2\hat{x}f_2'(-\hat{t}) + \frac{(\gamma_f - 1)}{(\pi Pr)^{\frac{1}{2}}} \int_0^{\hat{t}} \frac{f_2(-\tau)}{(\hat{t} - \tau)^{\frac{3}{2}}} \left[ \left( 1 - \frac{Pr\hat{x}^2}{2(\hat{t} - \tau)} \right) \exp\left( \frac{-Pr\hat{x}^2}{4(\hat{t} - \tau)} \right) - 1 \right] d\tau, \quad (4.7)$$

where

$$\theta_2(\hat{x}, \hat{t}) = (\gamma_f - 1) \left( \frac{Pr}{\pi} \right)^{\frac{1}{2}} \int_0^{\hat{t}} \frac{f_2(-\tau)\hat{x}}{(\hat{t} - \tau)^{\frac{3}{2}}} \exp\left( \frac{-Pr\hat{x}^2}{4(\hat{t} - \tau)} \right) d\tau.$$

Similar expressions for density and temperature apply.

#### 4.2. Thermal-boundary-layer effects on the interaction region

As  $\hat{x} \rightarrow -\infty$ , the asymptotic values of  $\theta_1(\hat{x}, \hat{t})$  and  $\theta_2(\hat{x}, \hat{t})$  in (4.4) and (4.6), respectively, tend to zero exponentially. Hence, as  $\hat{x} \rightarrow -\infty$ , for the fully and partly dispersed cases,  $\hat{T}^{(1)} \rightarrow 2(\gamma_f - 1)f_{1,2}'(-\hat{t})$  and  $\hat{\rho}^{(1)} \rightarrow 2f_{1,2}(-\hat{t})$ , which shows there is no effect on the temperature and density in the interaction region. However, the asymptotic value of thermal-layer velocity shows there are second-order effects. Writing (4.5) and (4.7) in co-ordinates  $(x, t)$  we find that, as  $\hat{x} \rightarrow -\infty$ ,

$$\hat{c}\hat{u}^{(1)} \rightarrow 2f_{1,2}'(-t)x + \hat{c}U_{1,2}(t),$$

where, for the fully and partly dispersed cases,

$$U_1(t) = -\frac{2(\gamma_f - 1)}{(\pi Pr)^{\frac{1}{2}}} \int_0^\infty f_1'(-t + \tau) \frac{d\tau}{\tau^{\frac{1}{2}}},$$

and

$$U_2(t) = \frac{2(\gamma_f - 1)}{(\pi Pr)^{\frac{1}{2}}} \left( \frac{f_2(0)}{t^{\frac{1}{2}}} - \int_0^t f_2'(-t + \tau) \frac{d\tau}{\tau^{\frac{1}{2}}} \right).$$

Thus, a velocity of  $O(\hat{\epsilon})$  is induced by heat conduction to the wall; and the interaction and thermal-layer expansions can only be matched if the interaction expansion takes the form

$$u(x, t) = u^{(1)}(x, t) + \epsilon u^{(2)}(x, t) + \hat{\epsilon} u^{(3)}(x, t) + O(\epsilon^2, \hat{\epsilon}^2, \epsilon \hat{\epsilon}). \tag{4.8}$$

Here  $u^{(1)}$  and  $u^{(2)}$  have been found in § 3, and  $u^{(3)}$  is the contribution from end-wall heat conduction to be determined by a matching with the thermal-layer results. This is equivalent to a new wall boundary condition for velocity determined by  $U_{1,2}(t)$ . (Here we take  $\hat{\epsilon} \gg \epsilon^2$ ; if  $\hat{\epsilon} \lesssim \epsilon^2$ , the induced velocity is  $O(\epsilon^2)$  and its influence negligible.) Substitution of (4.8) and similar expansions for other gas properties into the governing equations yields

$$\left( 1 + \frac{\partial}{\partial t} \right) (u_{tt}^{(3)} - u_{xx}^{(3)}) = 0.$$

For the fully dispersed case, the solution satisfying the condition that, as  $x \rightarrow 0$ ,  $u^{(3)} \rightarrow U_1(t)$  and the condition that, as  $t \rightarrow -\infty$  with  $x - t$  fixed,

$$u^{(3)}(x, t \rightarrow -\infty) \rightarrow 0$$

is of the form

$$u^{(3)}(x, t) = U_1(x + t). \tag{4.9}$$

This result shows that only a left-going wave is generated by the existence of the thermal boundary layer; the reflexion of this second-order wave from the ‘shock front’ is of higher order, and no right-going wave appears. The generated wave has the same ‘shape’ as the wall velocity  $U_1(t)$ . Similarly, we find that, for the partly dispersed case, the solution is  $u^{(3)} = 0$  for  $x + t < 0$  and

$$u^{(3)}(x, t) = U_2(x + t) \quad \text{for } x + t \geq 0. \tag{4.10}$$

The velocities at  $x = 0$  are not equal to zero; the new boundary values

$$\hat{\epsilon} u^{(3)}(0, t) = \hat{\epsilon} U_{1,2}(t)$$

are ‘effective wall velocities’. This corresponds to a flux of gas from the interaction region toward the end wall as a result of the hot gas adjacent to the wall being cooled by it. Integrating  $U_1(t)$  or  $U_2(t)$  gives the ‘effective wall displacements’

$$\hat{\epsilon} X_1(t) = \frac{\hat{\epsilon} 2(\gamma_f - 1)}{(\pi Pr)^{\frac{1}{2}}} \int_0^\infty f_1(-t + \tau) \frac{d\tau}{\tau^{\frac{1}{2}}},$$

and

$$\hat{\epsilon} X_2(t) = \frac{\hat{\epsilon} 2(\gamma_f - 1)}{(\pi Pr)^{\frac{1}{2}}} \left[ 2t^{\frac{1}{2}} f_2(0) - \int_0^t d\xi \int_0^\xi f_2'(-\xi + \tau) \frac{d\tau}{\tau^{\frac{1}{2}}} \right].$$

Figures 4 and 5 show the ‘effective wall velocities and displacements’ as functions of time, and delineate their asymptotic behaviour.

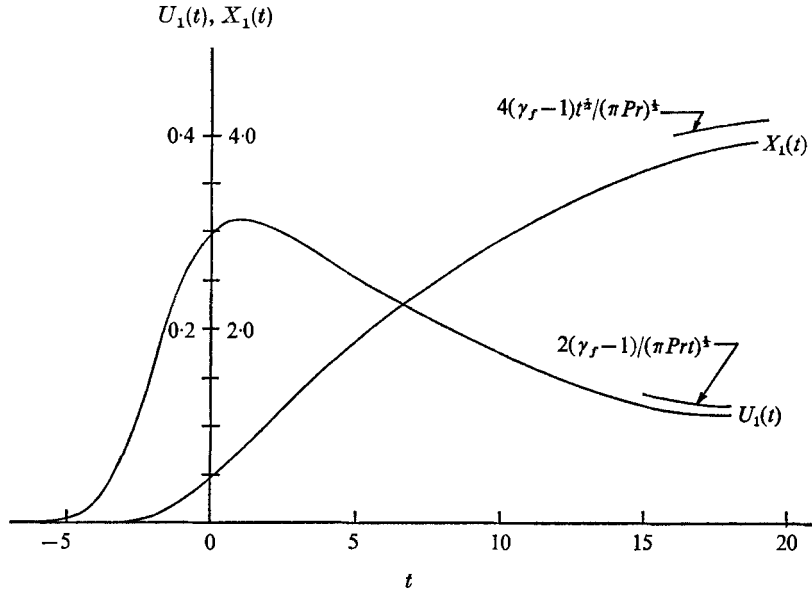


FIGURE 4. Effective wall velocity and displacement for fully dispersed shock ( $Pr = 0.75$ ,  $\kappa = 1.0$ ).

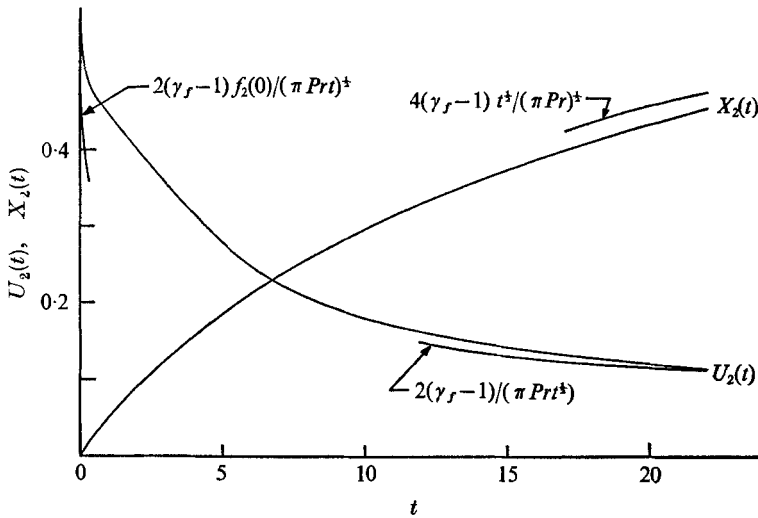


FIGURE 5. Effective wall velocity and displacement of partly dispersed shock ( $Pr = 0.75$ ,  $\kappa = 0.5$ ).

4.3. Thermal-layer effects on the reflected shock

We now turn to the problem of determining the effect of the thermal layer on the reflected shock after it has travelled many relaxation lengths. The new matching condition for the outer solution is that, as  $\bar{t} \rightarrow 0$ ,

$$\bar{u} = 1 - f_{1,2}(-\eta) - \left( \frac{5 - 3\gamma_f}{4} + \kappa \right) \bar{t} f'_{1,2}(-\eta) + \hat{e} U_{1,2}(\eta). \tag{4.11}$$

In §3 we noted that, in both the fully and partly dispersed cases, the first-order terms of (4.11) lead to a steady-state solution. Here we determine the influence of the term which accounts for end-wall heat conduction  $\hat{\epsilon}U_{1,2}(\eta)$  on the reflected shock trajectory. This requires the solution of (3.7) subject to the initial condition that, as  $\bar{t} \rightarrow 0^+$ ,

$$\bar{u} \rightarrow 1 - f_{1,2} \left( -\eta + \left( \frac{5 - 3\gamma_f}{4} + \kappa \right) \bar{t} \right) + \hat{\epsilon}U_{1,2}(\eta).$$

Equation (3.7) cannot be solved analytically. Owing to the complexity of  $U_{1,2}(\eta)$ , the asymptotic behaviour of  $\bar{u}$  is also difficult to find and we resort to a simple numerical method.

We introduce the co-ordinates

$$r = \eta - \left( \frac{1}{4}(5 - 3\gamma_f) + \kappa \right) \bar{t}, \quad \bar{t} = \bar{t}$$

and write

$$\bar{u}(r, \bar{t}) = 1 - f_1(-r) + \hat{\epsilon}\bar{u}^{(2)}(r, \bar{t}).$$

In these co-ordinates and with  $\bar{u}^{(2)}$  as our basic unknown, the second-order equation (3.7) is rewritten for the fully dispersed case as

$$\left. \begin{aligned} \left( 1 + \frac{\partial}{\partial r} \right) Q + \kappa \frac{\partial \bar{u}^{(2)}}{\partial r} &= 0, \\ \frac{\partial \bar{u}^{(2)}}{\partial \bar{t}} &= Q - \frac{\partial}{\partial r} (g_1 \bar{u}^{(2)}) - \hat{\epsilon} \frac{\gamma_f + 1}{2} \bar{u}^{(2)} \frac{\partial \bar{u}^{(2)}}{\partial r}, \end{aligned} \right\} \quad (4.12)$$

subject to the initial condition  $\bar{u}^{(2)}(r, 0) = U_1(r)$ , where

$$g_1(r) = - \left( \frac{\gamma_f + 1}{4} + \kappa \right) + \frac{\gamma_f + 1}{2} (1 - f_1(-r)).$$

Solving the first equation for  $Q(r, t)$  for given  $\bar{u}^{(2)}(r, \bar{t})$  with  $Q(-\infty, \bar{t}) = 0$  at a given time  $\bar{t} = \bar{t}_0$ , then substituting the result into the second equation, we may determine  $\bar{u}^{(2)}(r, \bar{t} + \Delta\bar{t})$ . For stability, an ‘up-wind’ differencing scheme is used. In our case, the term  $g_1(r) \partial \bar{u}^{(2)} / \partial r$  is written in forward differences and  $\bar{u}^{(2)} u_r^{(2)}$  in backward differences.

For the partly dispersed case, the basic numerical scheme is the same except that special techniques are required at the shock front. The speed of the shock front and the conditions right behind it are not known *a priori*. In this case, it is convenient to write the dependent variable for velocity in the form

$$\bar{u}(r, \bar{t}) = 1 - f_2(-r + r_s(\bar{t})) + \hat{\epsilon}\bar{u}^{(2)}(r, \bar{t}), \quad (4.13)$$

where  $r_s(\bar{t})$  is an unknown function of time  $\bar{t}$  to be computed by knowing the shock speed at any instant. The discontinuous jump is at  $r - r_s(\bar{t}) = 0$ , and the local shock speed is

$$U^*(\bar{t}) = - \left[ 1 - \left( \frac{5 - 3\gamma_f}{4} + \kappa \right) \epsilon \right] a_{f0} + \epsilon a_{f0} \frac{dr_s(\bar{t})}{d\bar{t}},$$

while the velocity right behind the shock front is  $\bar{u}_s = 1 - f_2(0) + \hat{\epsilon}\bar{u}_s^{(2)}(\bar{t})$ , where  $\bar{u}_s^{(2)}(\bar{t})$  denotes the jump of the second-order term. The Rankine–Hugoniot relations require

$$\frac{dr_s(\bar{t})}{d\bar{t}} = \hat{\epsilon} \frac{\gamma_f + 1}{4} \bar{u}_s^{(2)}(\bar{t}), \quad (4.14)$$

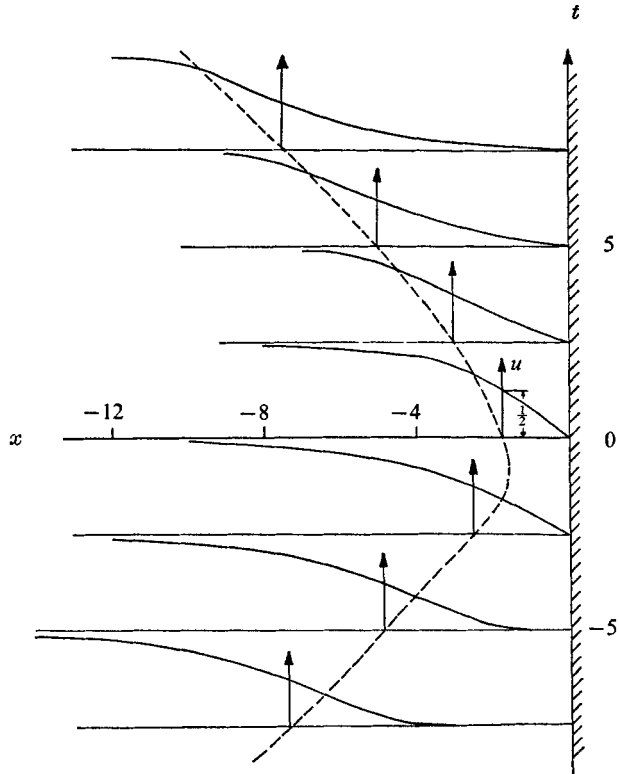


FIGURE 6. Velocity profiles near an adiabatic wall. ---, locus of points where  $u = 0.5$ . ( $\epsilon = 0.01$ ,  $\kappa = 1.0$ .)

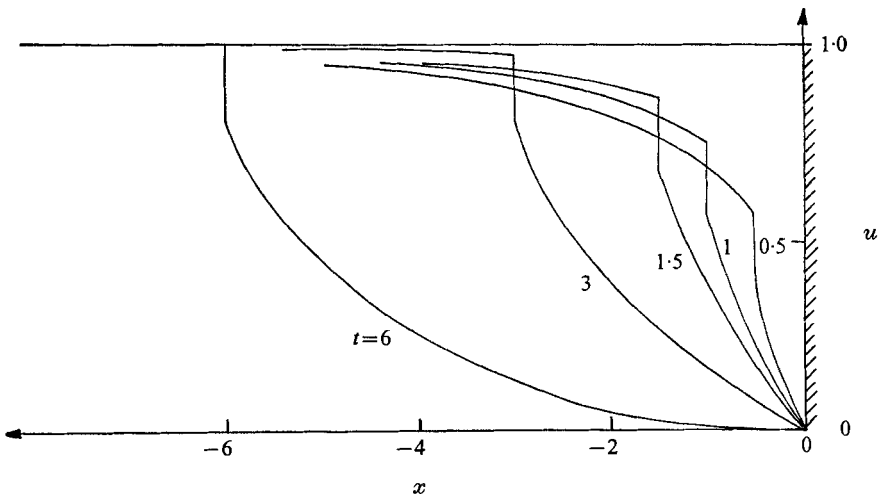


FIGURE 7. Reflected velocity profiles for partly dispersed wave (adiabatic wall). ( $\epsilon = 0.01$ ,  $\kappa = 0.5$ .)

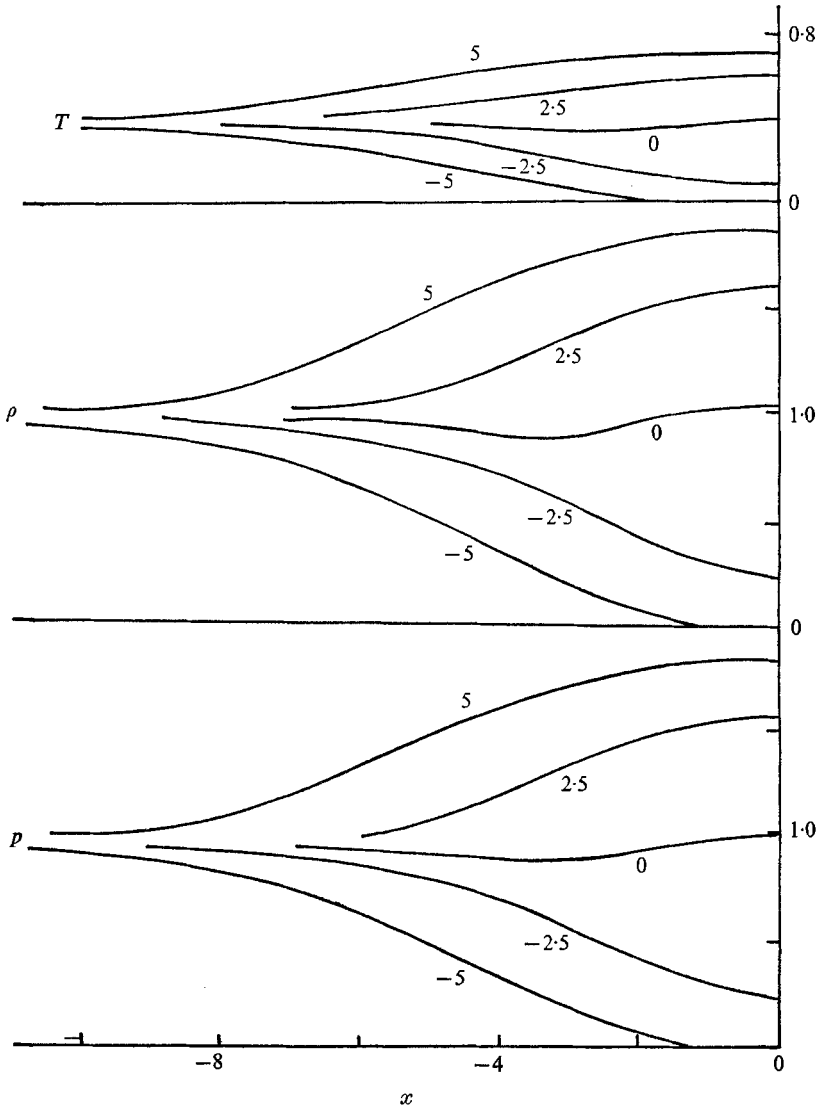


FIGURE 8. Flow-field properties of a fully dispersed wave during the reflexion from an adiabatic wall ( $\epsilon = 0.01$ ,  $\kappa = 1.0$ ). (Curves labelled with values of  $t$ .)

which provides us with the relation for calculating  $r_s(\bar{t})$  and then determining the shock position  $x_{\text{shock}}^*$  for all times  $t^*$ . Substitution of (4.12) into (3.7) yields equations similar to (4.13).

The grid points for the finite differences are designated such that the node points have equal spacing except in the first mesh, which is affected by shock position. At time  $\bar{t}$ , we solve the analogue of the first of (4.12) for  $Q(r, \bar{t})$  given  $\bar{u}^{(2)}(r, \bar{t})$  with  $Q(r = r_s(\bar{t}), \bar{t})$  evaluated from the analogue of the second of (4.12). We then substitute  $Q(r, \bar{t})$  into the analogue of the first of (4.12) to compute  $\bar{u}^{(2)}(r, \bar{t} + \Delta\bar{t})$ . Using (4.14) we calculate  $r_s(\bar{t} + \Delta\bar{t})$ , then find  $\bar{u}^{(2)}(r = r_s(\bar{t} + \Delta\bar{t}), \bar{t} + \Delta\bar{t})$  by linear interpolation.

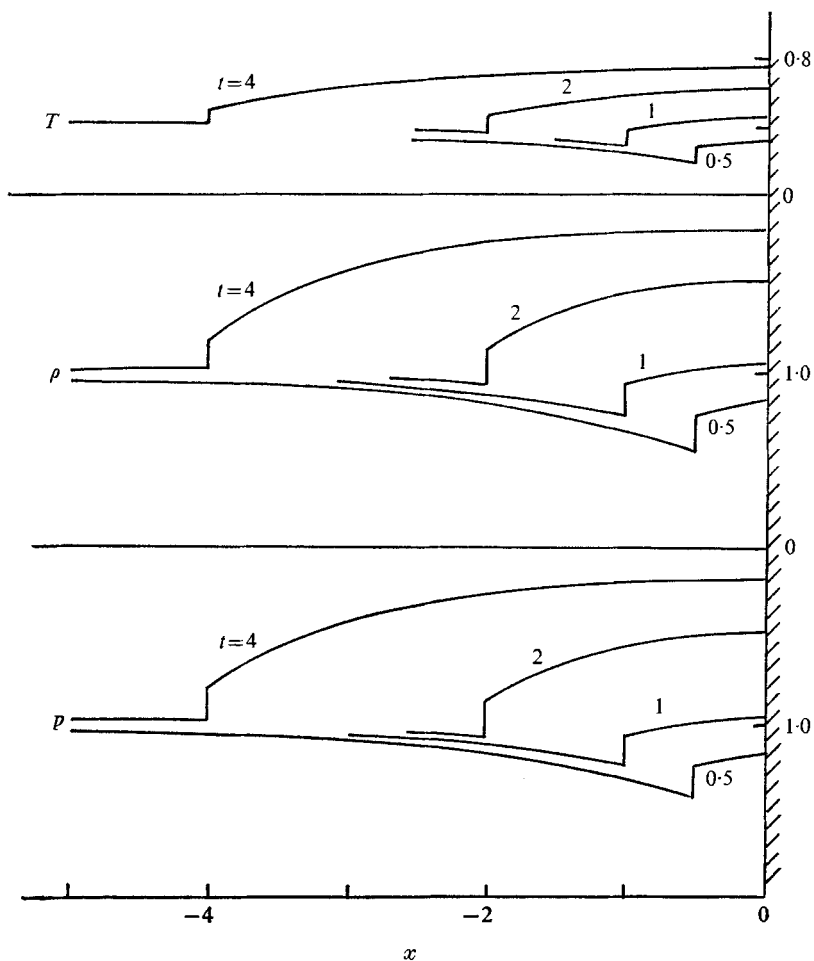


FIGURE 9. Flow-field properties of a partly dispersed wave during the reflexion from an adiabatic wall ( $\epsilon = 0.01$ ,  $\kappa = 0.5$ ).

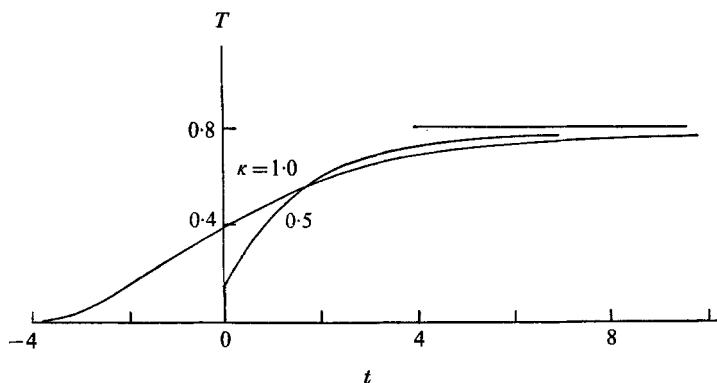


FIGURE 10. Adiabatic end-wall temperature history ( $\epsilon = 0.01$ ,  $\gamma_f = 1.4$ ).

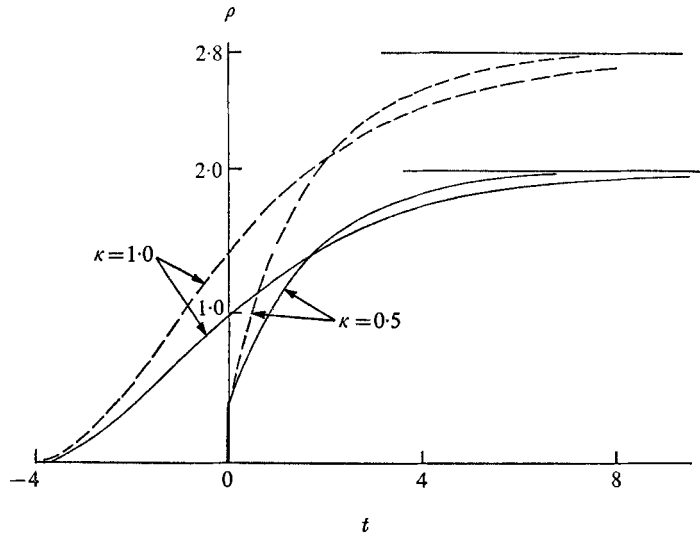


FIGURE 11. Comparison of the end-wall density history for adiabatic (—) and isothermal (---) walls.

## 5. Discussion and and conclusion

The analytical results of our work are given in §§ 3 and 4. While they provide an understanding of the resulting phenomena, they are more easily interpreted after they have been evaluated numerically for some specific case. Unfortunately, we have not found appropriate experimental results for comparison; since weak shock waves have been studied in the absence of vibrational relaxation and moderate strength shock waves with vibrational relaxation examined, such experiments are possible. Increased interest in diverse vibrational relaxation times seems likely to lead to such experiments. The appropriate analytical results can be computed from the appropriate composite expansions given in § 4. Here we illustrate some of these for an arbitrarily chosen weak shock strength. Flow fields are computed for both fully and partly dispersed shock waves corresponding to initial frozen Mach numbers smaller and greater than one. The Prandtl number is taken to be 0.75 and  $\gamma_f = 1.4$ ; these values are appropriate for a vibrationally relaxing diatomic gas.

Figure 6 shows the spatial variation of velocity for a fully dispersed shock wave constructed from the composite expansion for the adiabatic wall problem. These curves show the interaction between the shock wave and the end wall. The dashed lines represent the trajectory of the points where  $u = \frac{1}{2}$ , which we may take to be the location of the shock. The shock wave comes from the left with non-dimensional speed  $1 + (\frac{1}{4}(\gamma_f + 1) - \kappa)\epsilon$ , is reduced to zero speed then reflected back with a speed that approaches  $1 - (\frac{1}{4}(5 - 3\gamma_f) + \kappa)\epsilon$ . Near the wall the flow velocity must vanish, and the balance between convection and 'relaxation' dispersion, which maintains the profile of a steady-state shock wave, cannot continue to hold. The first-order solution agrees with an acoustic approximation, behaving like the interaction of two weak waves with equal strengths but moving



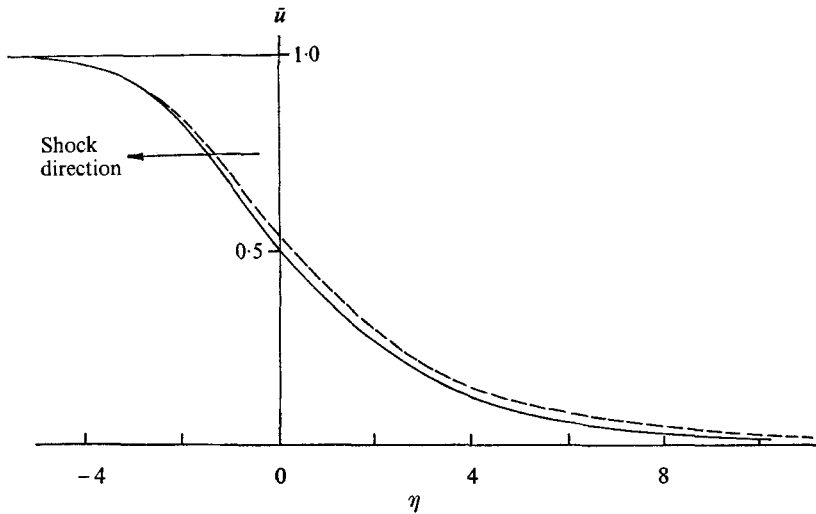


FIGURE 12. Velocity profile of a fully dispersed shock wave reflected from an isothermal wall ( $\bar{i} \rightarrow 0$ ). - - - -, includes induced thermal velocity ( $\hat{\epsilon} = 0.1, \kappa = 1.0$ ).

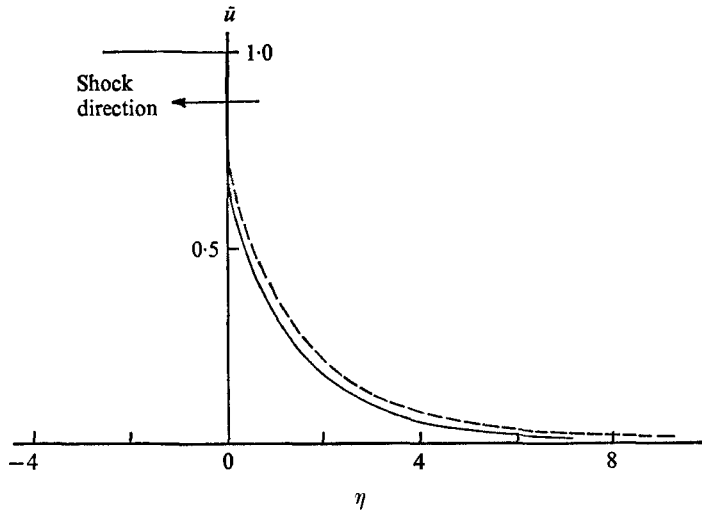


FIGURE 13. Velocity profile of partly dispersed shock wave reflected from an isothermal wall ( $\bar{i} \rightarrow 0$ ). - - - -, includes induced thermal velocity. ( $c = \hat{\epsilon} = 0.1, \kappa = 0.4$ .)

in opposite directions. Convection and dispersion fail to balance to second order. For a partly dispersed wave, the wave consists of a Rankine-Hugoniot jump followed by a relaxation zone. Since a partly dispersed shock wave propagates faster than the frozen sound speed, there is no interaction with the wall before it reaches the wall. Figure 7 shows the velocity profiles of a partly dispersed shock wave after reflexion from an adiabatic wall. Figures 8 and 9 are plots of the variation in pressure, density and temperature, during reflexion from an adiabatic wall. The derivatives of these thermodynamic properties are always zero at the wall, and the properties always have extreme values there. Figure 10 depicts the value of the time-varying adiabatic-end-wall temperature.

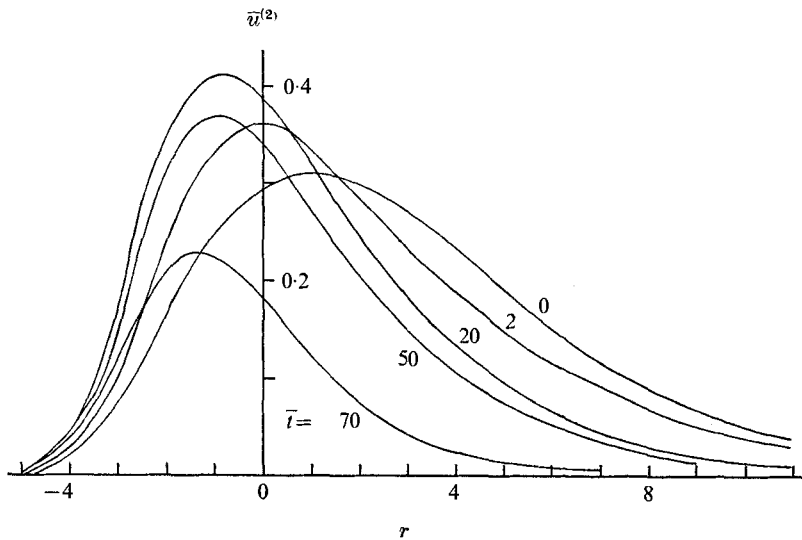


FIGURE 14. Variation of induced thermal velocity, fully dispersed shock ( $\hat{\epsilon} = 0.01$ ,  $\kappa = 1.0$ ).

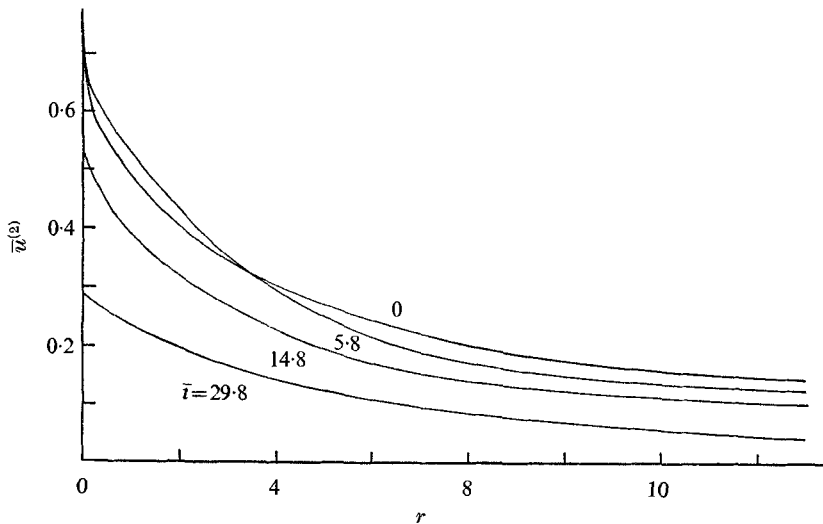


FIGURE 15. Variation of induced thermal velocity, partly dispersed shock ( $\epsilon = 0.01$ ,  $\hat{\epsilon} = 0.02$ ,  $\kappa = 0.4$ ).

For an isothermal wall, there is a thermal layer with thickness  $O(R_{a_f}^{\frac{1}{2}} \tau^*)$ . The pressure is approximately constant through this thin thermal layer, while the gas is cooled and thus density increased. The pressure at the isothermal end wall is the same as that at the adiabatic wall. Figure 11 shows the values of density at adiabatic and isothermal walls as functions of time. The existence of the thermal boundary layer does not affect the incoming steady-state shock, but does affect the structure of the reflected shock to  $O(R_{a_f}^{\frac{1}{2}} \tau^*)$ . The 'negative' thermal layer attenuates the strength of the reflected shock wave. Figures 12

and 13 demonstrate the effect of this induced thermal velocity on the structure of the reflected shock wave. The influence of induced velocity is comparatively more profound, and exists longer, in the region far behind the wave front. Figures 14 and 15 show the details of the time variation of the induced thermal velocity in the reflected far-field region. For large times, the effects of the thermal layer become weaker and the structure of the shock wave returns to the steady structure, which represents a balance between nonlinear convection and relaxation dispersion.

This research was supported by the U.S. Air Force Office of Scientific Research. The authors are indebted to Professors W. R. Sears and E. L. Resler for their suggestions and helpful discussions. They are also indebted to the referees and to Dr H. Buggisch for particularly constructive criticisms of the manuscript.

## REFERENCES

- BAGANOFF, D. 1965 *J. Fluid Mech.* **23**, 209.  
 BECKER, E. 1970 *Aeronautical J.* **74**, 736.  
 BETHE, H. A. & TELLER, E. 1941 *Aberdeen Proving Ground BRL Rep. X-117*.  
 BLYTHE, P. A. 1969 *J. Fluid Mech.* **37**, 31.  
 BRANDON, H. J. 1969 Nonequilibrium flow fields behind reflected shock waves. Ph.D. thesis, Washington University.  
 BROER, L. J. F. 1951 *Appl. Sci. Res.* **A2**, 447.  
 BUGGISCH, H. 1969 *Z. angew. Math. Mech.* **49**, 495.  
 BUGGISCH, H. 1970 *Z. angew. Math. Mech.* **50**, T168.  
 CLARKE, J. F. 1967 *Proc. Roy. Soc.* **A299**, 221.  
 CLARKE, J. F. & MCCHESENEY, M. 1964 *The Dynamics of Real Gases*. Butterworths.  
 FREEMAN, N. C. 1958 *J. Fluid Mech.* **4**, 407.  
 GLASSMAN, I. 1966 *Recent Advances in Aerothermochemistry, AGARD Conf. Proc.* **12**, vol. 2.  
 GOLDSWORTHY, F. A. 1959 *J. Fluid Mech.* **5**, 164.  
 GUNN, J. C. 1946 *Aero. Res. Council. R. & M.* no. 2338.  
 HANSON, R. K. 1971a *J. Fluid Mech.* **45**, 721.  
 HANSON, R. K. 1971b *A.I.A.A. J.* **9**, 1811.  
 JOHANNESSEN, N. H., BIRD, G. A. & ZIENKIEWICZ, H. K. 1967 *J. Fluid Mech.* **30**, 51.  
 LESSER, M. B. & SEEBASS, A. R. 1968 *J. Fluid Mech.* **31**, 501.  
 LIGHTHILL, M. J. 1956 *Surveys in Mechanics* (ed. G. K. Batchelor & R. Davis), pp. 250-351. Cambridge University Press.  
 OCKENDON, H. & SPENCE, D. A. 1969 *J. Fluid Mech.* **39**, 329.  
 PRESLEY, L. L. & HANSON, R. K. 1968 *A.I.A.A. J.* **7**, 2267.  
 SPENCE, D. A. 1961 *Proc. Roy. Soc.* **A264**, 221.  
 STURTEVANT, B. & SLACHMUYLDERS, E. 1964 *Phys. Fluids*, **7**, 1201.  
 VAN DYKE, M. D. 1964 *Perturbation Methods in Fluid Mechanics*. Academic.  
 VINCENTI, W. G. & KRUGER, C. H. 1965 *Introduction to Physical Gas Dynamics*. Wiley.